ANALYSIS OF CONCRETE STRUCTURES ACROSS THE DUCTILITY SPECTRUM

Wendel SEBASTIAN Chao ZHANG

Department of Civil Engineering, University of Bristol, UK

Keywords: Concrete, Ductility, Failure, FRP, Iterative, Linear Analysis, Redistribution.

1 INTRODUCTION

The lower bound theorem of plasticity underpins traditional design of statically indeterminate reinforced concrete (RC) structures via the procedure outlined in Fig. 1(a). Uncracked analyses for ultimate load cases are followed by dimensioning and / or reinforcement detailing – with moment redistribution for less onerous detailing – to give sufficient ductility via steel yield at peak moment locations. The ductility guarantees sufficient actual moment redistribution capability for the design loads to be achieved and so no checks on load capacity are required for the detailed structure.

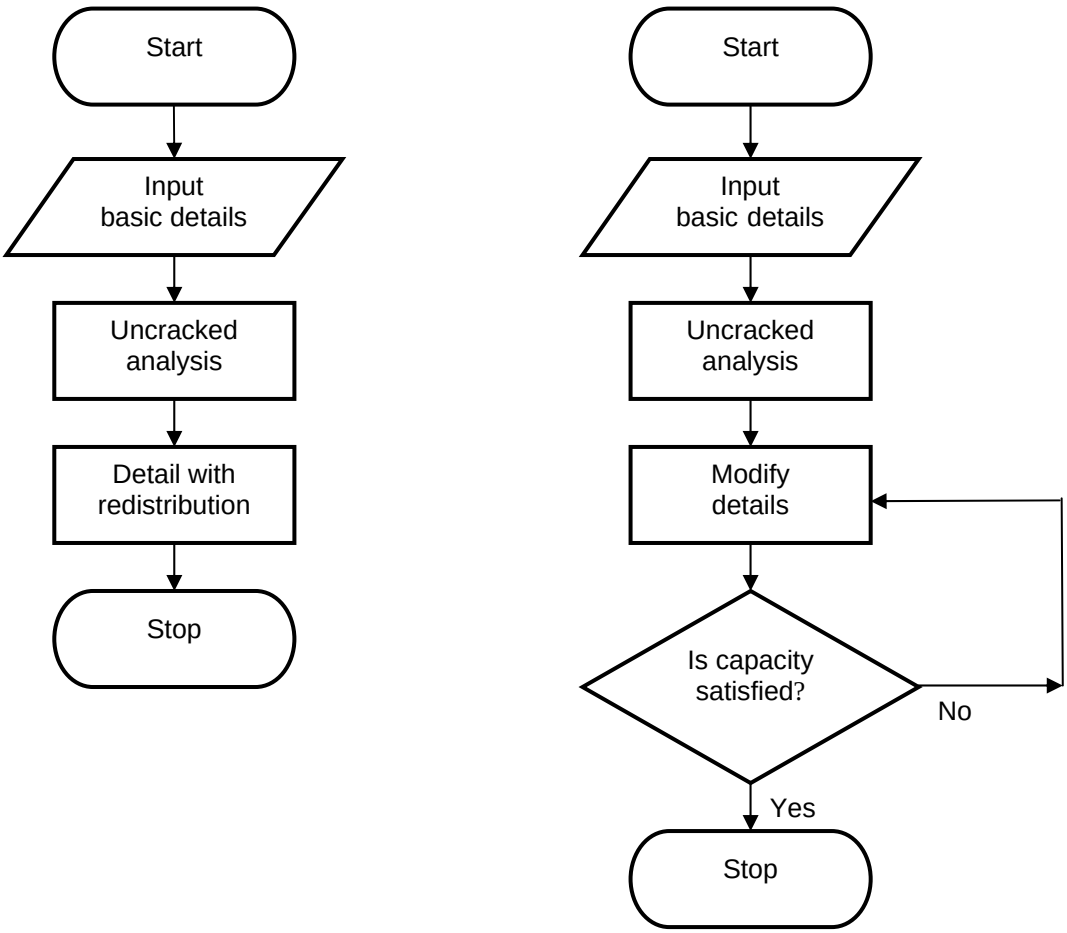

(a) Existing approach **(b)** New Approach

Fig. 1 – Design of Indeterminate Reinforced Concrete Structures

If the structure is ductility-deficient, then detailing to uncracked analysis and redistribution may be unsafe, so an alternative approach is needed. One such approach, outlined in Fig. 1(b), entails an iterative loop where analysis is conducted to quantify the load capacity of the detailed structure, with

any deficiency in capacity triggering a re-detailing of the structure. The capacity analysis must account for nonlinearities in the structure at ultimate and still be time-efficient in a design environment, while the re-detailing procedure must permit rapid convergence onto load capacity. This paper presents a potentially time-efficient method for the capacity analysis.

This analysis must apply whatever the structure's ductility. Now the moments developed by an indeterminate structure under load depend on the flexural stiffness (EI) distribution of the structure under that load. For an RC structure, the EI distribution in return depends on the moments. Thus, the capacity analysis must identify a load level at which the EI distribution gives moments consistent with that distribution and also at which the moment(s) at the critical location(s) correspond to failure. This idea underpins the present capacity analysis.

The crux of the analysis is the submission of an EI distribution to linear beam element analysis under the specified loads with a factor applied. Unless the moment distribution output from this analysis corresponds to the input EI distribution and just equates to section capacity at the critical location(s), then the EI distribution and load must be adjusted for repeat of the analysis. In this study, these adjustments are based on factoring the critical moment (here defined as that giving the highest ratio relative to section capacity) to equate to section capacity. The factor used to achieve this is also applied to the entire moment distribution of the structure and to the load. The EI distribution corresponding to this factored moment distribution is input to the analysis with the new factored loading and the process is repeated until the EI – moment convergence and the failure condition are both satisfied. In this manner, an iterative use of the EI distribution is used to predict capacity. The first iteration uses the uncracked EI distribution, with cracked / yield EI values used in subsequent iterations according to the moments which emerge from analysis. The EI values are the secant gradients of the moment-curvature relations. Prakhya and Morley [1] have comprehensively demonstrated how these moment-curvature relations can be influenced by tension stiffening in the cracked concrete.

Constant EI is assumed along a typical beam element. Thus, the general nonlinear variation of section flexural stiffness anticipated along peak moment zones at ultimate must be approximated in a piecewise linear manner in the analysis ; finer beam element meshes giving better approximations to the true EI distributions and failure loads. In the remainder of this paper, this capacity prediction method is applied to 3 different structures – of differing ductilities – reinforced with either strain hardening steel or with fibre reinforced polymer (FRP) and perfectly plastic steel. Two continuous beam structures with different boundary conditions and a frame are considered. Where external FRP reinforcement is used, loss of ductility can be due to separation of the FRP from the concrete as reported primarily in the Conference Proceedings edited by Burgoyne [2] and in other work [3 - 6]. Alternatively, if appropriate FRP-to-concrete anchorage is provided, section failure occurs by concrete crushing or by rupture of the FRP. Even so, reduced ductility exists owing to the linear constitutive behaviour of the FRP up to failure [7].

In the examples which follow both the steel and FRP are of Young's modulus 200 kN/mm^2, while the steel is of yield stress 460 N/mm^2 and is perfectly plastic unless stated otherwise. The FRP is assumed to be of rupture stress in excess of the maximum FRP stresses developed at failure of the structures concerned. Also, sufficient anchorage to prevent separation of the FRP from the concrete is assumed, so that failure always occurs by crushing of the concrete. The moment – curvature relations used henceforth are based on general nonlinear or multi-linear material behaviours for the concrete, steel and FRP. These relations can be found in and have been verified using published test data in [8].

2 ANALYTICAL STUDY

2.1 Example 1

The first example is shown in Fig. 2 and comprises a 300 mm wide, 2-span continuous beam with rotationally free ends. Only embedded steel reinforcement with a strain hardening modulus of 5 kN/mm^2 is used. The structure, but not the loading – a UDL on one span and a point load of half the UDL at the other midspan – is symmetric about the middle support. The hog and sag steel areas are 1950mm^2 and 1350mm^2 respectively. Moment – curvature relations for the different reinforced sections can be seen in Fig. 3. "D" refers to **d**oubly reinforced sections, "H" to a **h**ogging section, "S" to a **s**agging section. Hence "DS" refers to a **d**oubly reinforced section in **s**agging. All dimensions of Fig. 2 are in mm.

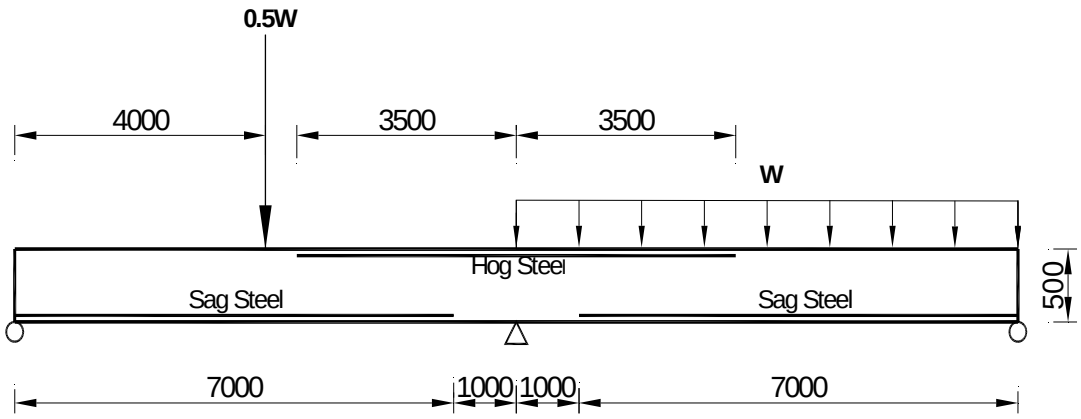

Fig. 2 – Two-span Continuous Beam with Rotationally Free Ends

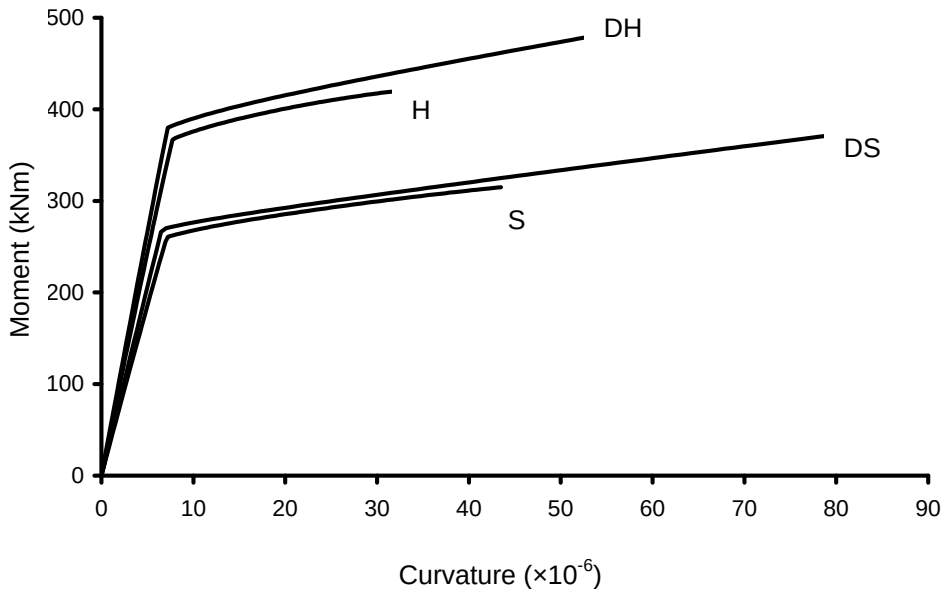

Fig. 3 – Moment – curvature plots

The analysis predicted moment failure over the central support at 58 kN/m UDL. Ten iterations gave convergence onto this load. This convergence coincided with attainment of moment – EI consistency and with the failure condition being satisfied. Fig. 4 shows the variation of normalised predicted failure load with iterations. Palpable oscillations of predicted load occurred during the first 5 iterations, with some stability thereafter. Fig. 5 shows, for iteration 5, the normalised EI distribution along the normalised length of the member. Extensive steel yield up to concrete crushing over the middle support and lesser steel yield not up to concrete crushing within the midspan under UDL account for the reduced EI values in those zones. The narrow zone of low EI over the middle support is due to the rapid fall-off of moment there while the yield zone in the UDL midspan region is wider owing to the low change of high moment along the parabolic moment variation there.

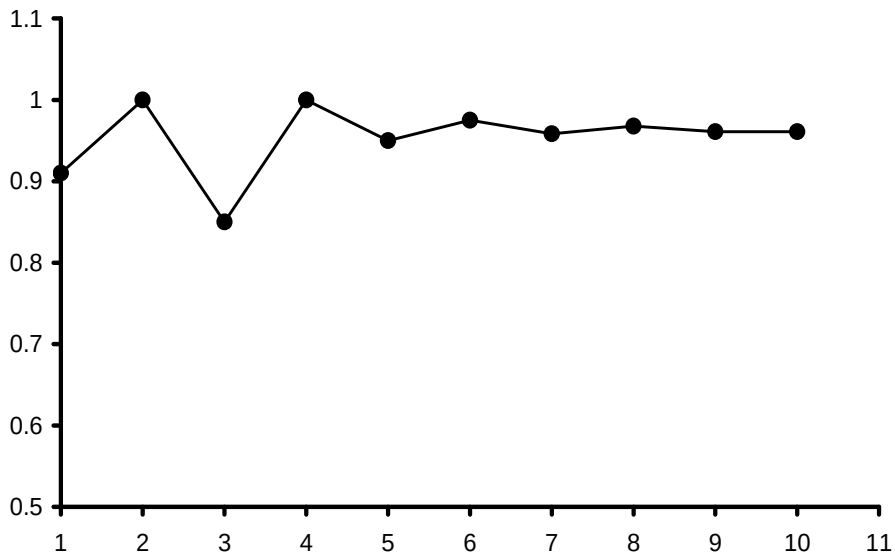

Fig. 4 – Variation of predicted load with iterations

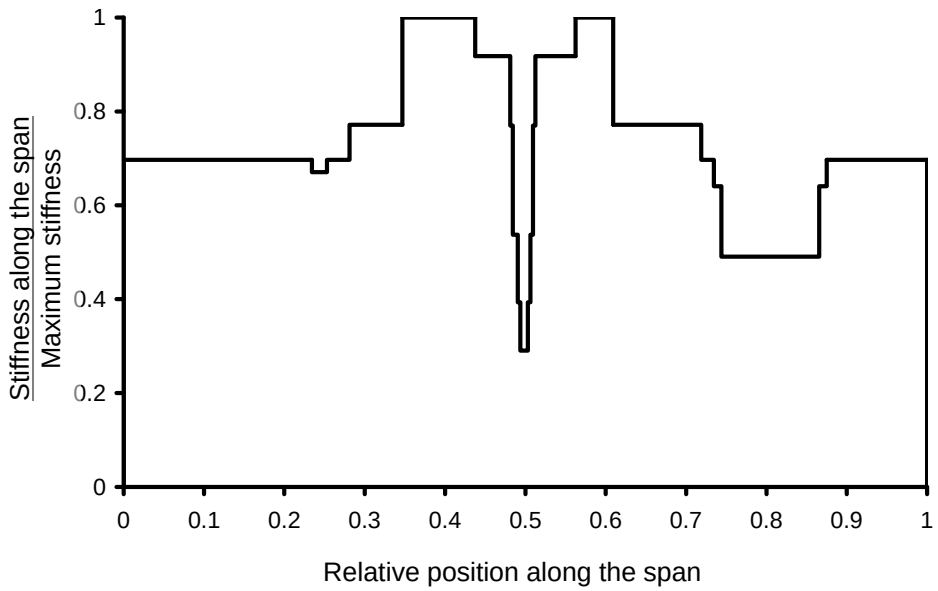

Fig. 5 – Normalised EI Distribution at Convergence

2.2 Examples 2, 3

This example, shown in Fig. 6, again comprises a 300 mm wide, 2-span continuous member, but this time with encastered ends and is reinforced with both steel and FRP. Again, the structure but not the loading is symmetric about the middle support. The use of a point load at each midspan – rather than a UDL and a point load as in Example 1 – make for different redistribution characteristics after first yield relative to Example 1. This is accentuated by the different ratio (0.75) between the two point loads relative to the value (0.5) used in Example 1. The hog FRP reinforcements at the ends are assumed to be adequately anchored (say, by embedment in the walls or other structures which provide the end restraints) to avoid FRP-steel separation. The hog and sag steel areas are 2550 mm^2 and 750 mm^2 respectively, while the hog and sag FRP areas are 36 mm^2 and 15 mm^2. These modest FRP areas give slightly rising moment – curvature characteristics after steel yield. Fig. 7 shows that the hogging sections ("H") have short ductility near-plateaux while the midspan sections are of significant ductility.

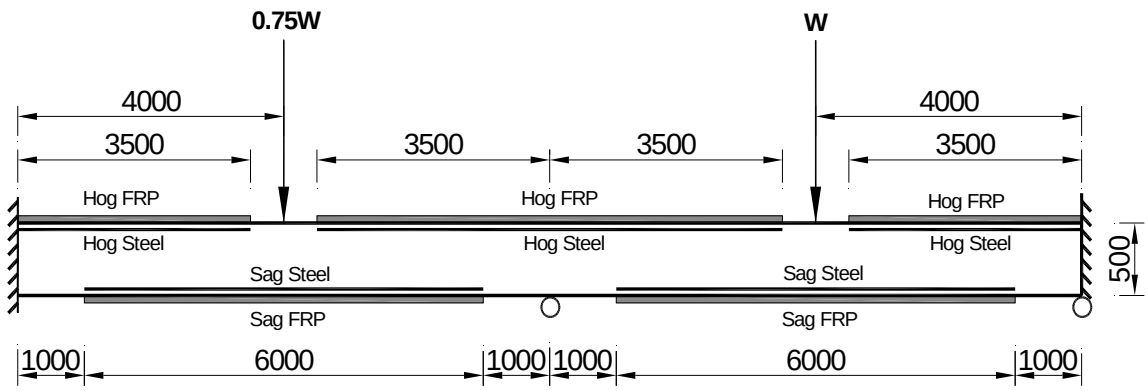

Fig. 6 – Two-span Continuous Beam with Encastered Ends

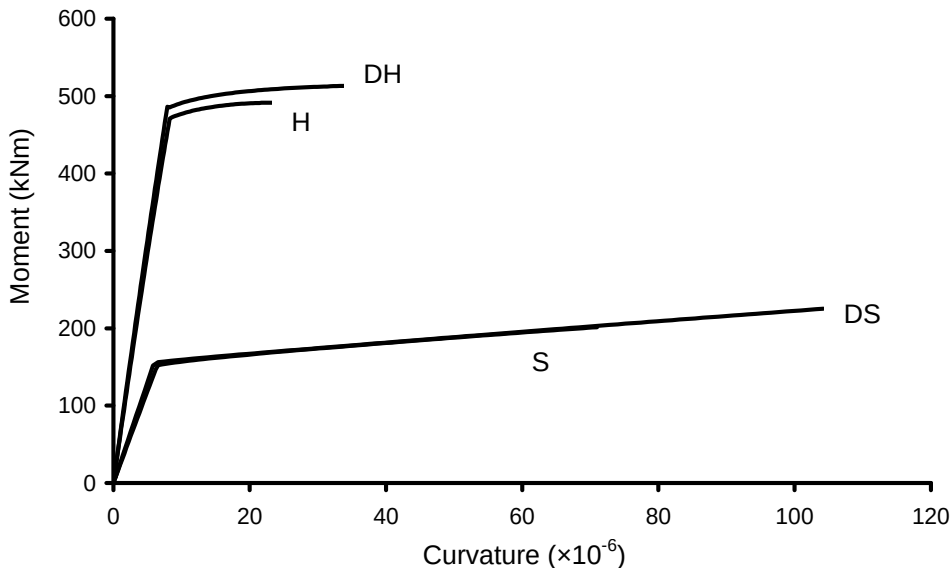

Fig. 7 – Moment – curvature plots

Fig. 8 shows that the analysis results oscillated significantly for the first 6 iterations, with convergence from the 7th to the 8th iteration. Fig. 9 gives the normalised EI distribution along the structure at the final predicted failure load of 312 kN, with predicted failure over the end support for the more heavily loaded span. Care was taken with the element mesh in zones of rapidly varying EI value to avoid ill-conditioning. This EI distribution represents extensive steel yield at the support of the more heavily loaded span and at midspan locations owing to the high sag moments generated by the point loads there ; the effect being more pronounced in the more heavily loaded span. Thus the significant length of the near-plateau in the more heavily loaded midspan zone permitted some ductile behaviour.

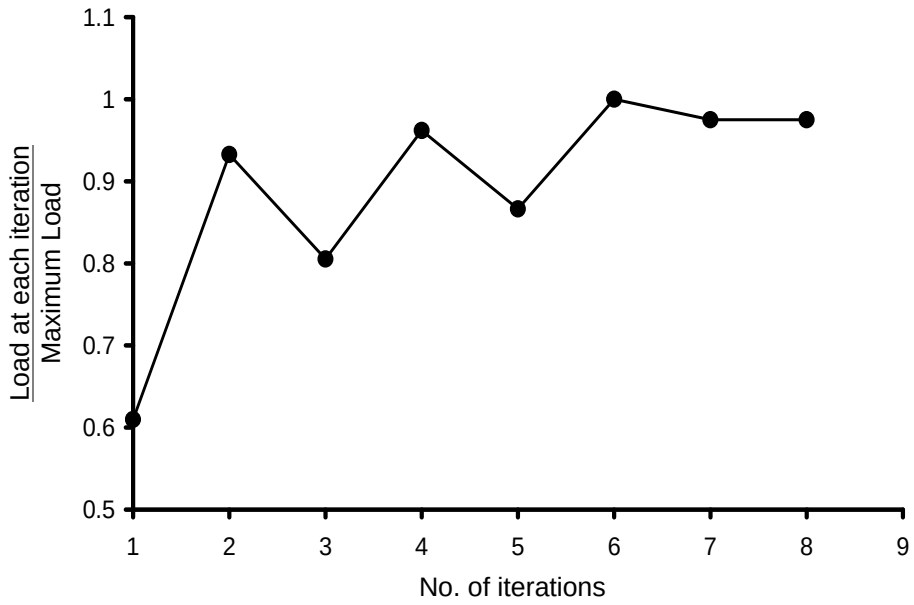

Fig. 8 – Variation of predicted failure load with iterations

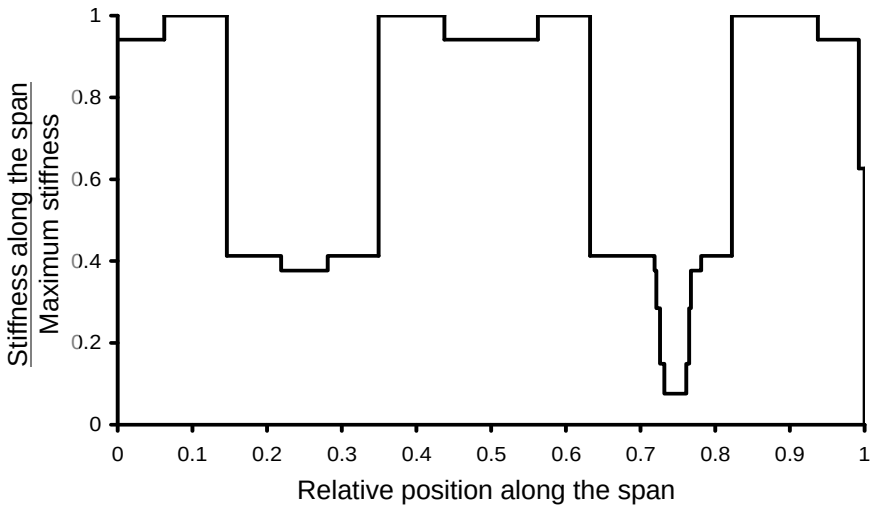

Fig. 9 – EI Distribution after final iteration

If, instead, the member is FRP strengthened to a significantly higher extent by increasing the FRP areas to 200 mm^2 and 350 mm^2, giving the significantly strain-hardened moment-curvature relations of Fig. 10, then the convergence characteristics of the iterative procedure change to that of Fig. 11. Fewer iterations are needed for convergence than previously, with lesser fluctuation of the predicted failure load (finally 492 kN). The normalised EI distribution at iteration 3, *en route* to convergence, is given in Fig. 12.

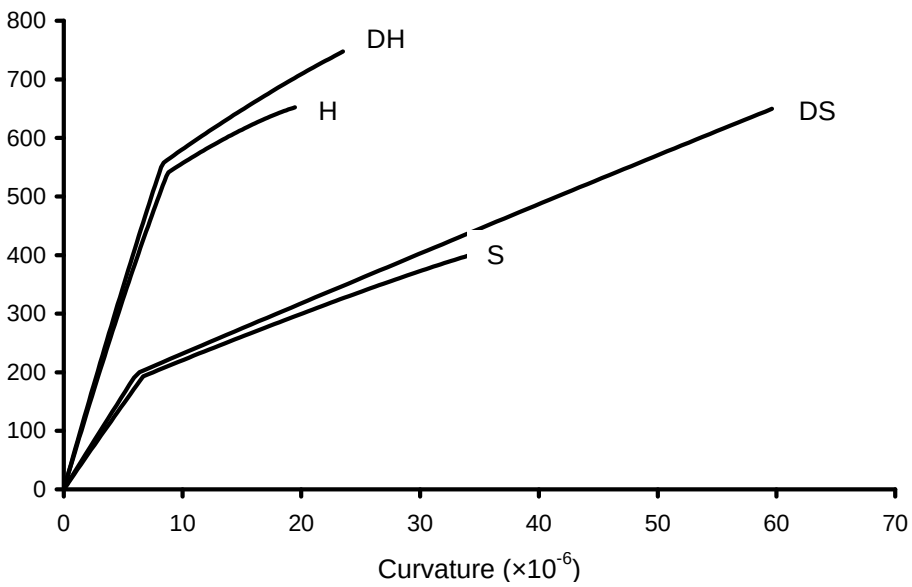

Fig. 10 – Moment – curvature plots

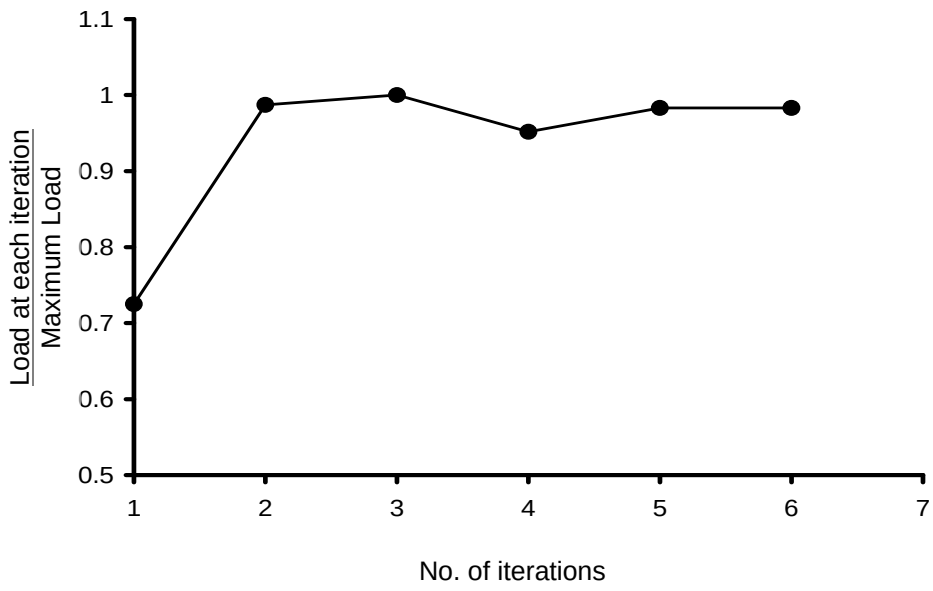

Fig. 11 – Variation of predicted failure load with iterations

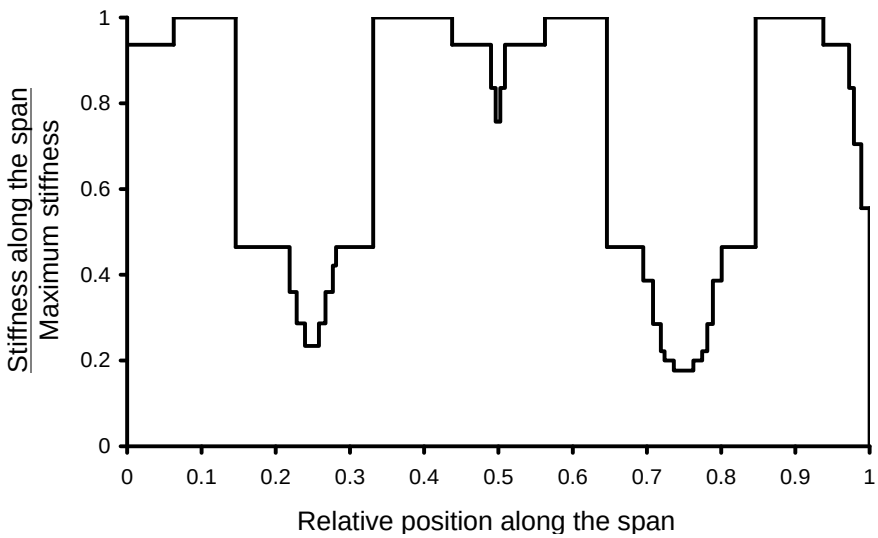

Fig. 12 – EI Distribution after iteration 3

2.3 Example 4

A 300 mm wide steel and FRP reinforced concrete frame under horizontal and vertical loads is considered in the final example, see Fig. 13. Again, adequate anchorage of the FRP is assumed on both the beam and the columns. The FRP and steel areas are given in brackets next to the relevant labels in the Figure. The significant FRP reinforcing leads to largely cracked linear behaviour up to failure. In this case only 4 iterations are needed to converge on to a failure state (predicted at 640kN) as shown in Fig. 14. Indeed, the second iteration is quite close to that final state and the iterations are stable thereafter, as may be expected from the minimal deviation from linear (though cracked) behaviour.

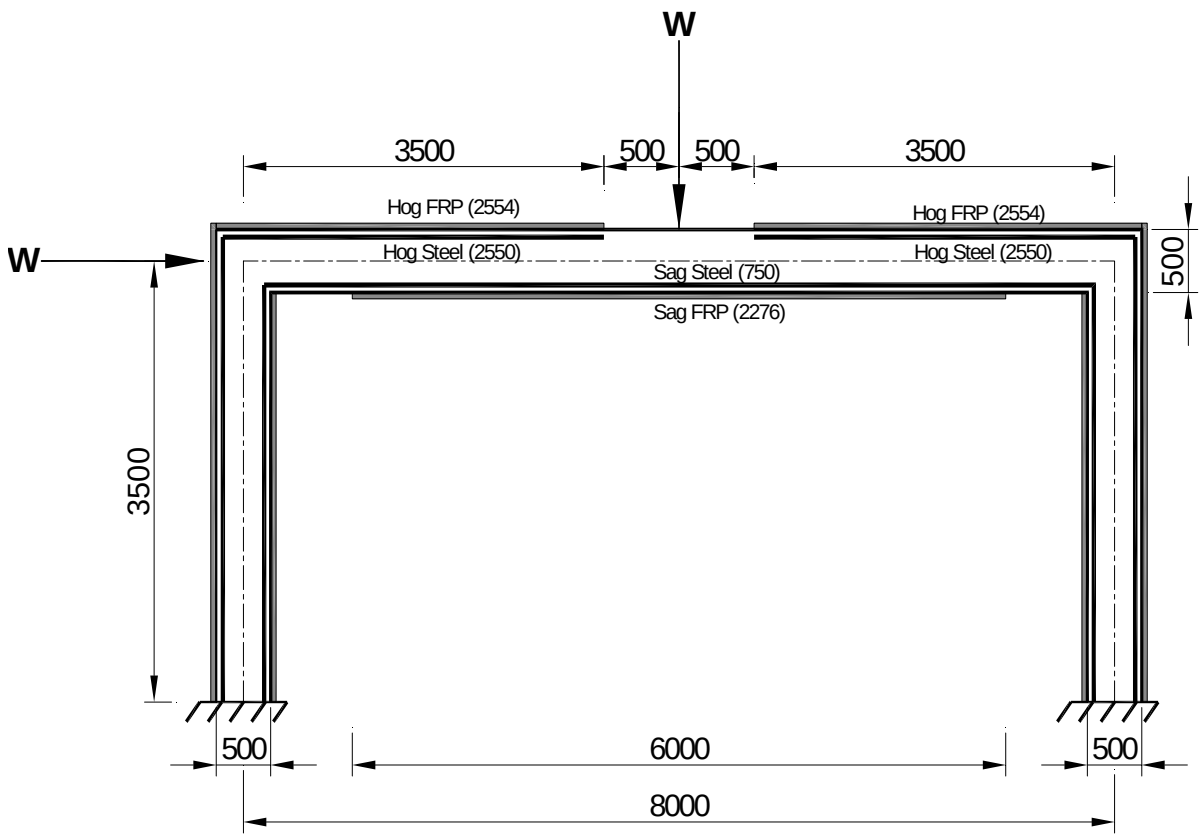

Fig. 13 – Frame with encastered feet

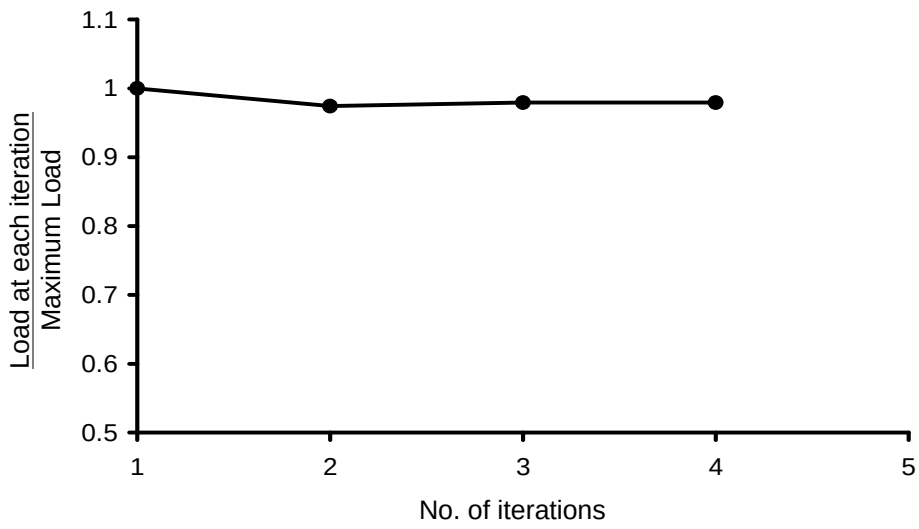

Fig. 14 – Variation of predicted failure load with iterations

3 CONCLUSIONS

The examples cover a range of structural ductilities under different types of loading. Attainment of convergence in each case thus suggests that this may well constitute a reliable technique for failure analysis prediction. Since linear beam analysis can be performed on standard structural analysis software, the method may be widely used. In addition, the technique gives useful insight into the influence of EI distributions on the moments developed in indeterminate RC structures under different loadings. The procedure may be extended to incorporate effects of states of self stress and to investigate behaviours in the pre-failure nonlinear regime of behaviour.

REFERENCES

[1] Prakhya, G.K.V. and Morley, C.T.M., "Tension Stiffening and Moment-Curvature Relations of Reinforced Concrete Elements", *ACI Structural Journal*, 87, 5, 1990, pp 597-605.

[2] Burgoyne, C. J., Editor, "Proceedings of the 5th International Symposium on Non-Metallic (FRP) Reinforcement for Concrete Structures, Volumes 1 and 2", 2001, Cambridge, published by Thomas Telford, London.

[3] Hutchinson, A. R., and Rahimi, H., ''Behavior of Reinforced Concrete Beams with Externally Bonded Fibre Reinforced Plastics.'' *Proc., 5th Int. Conf. on Struct. Faults and Rep.*, ECS, Edinburgh, U.K., 1993, pp 221–228.

[4] Hassanen, M. A. H. and Raoof, M., "Design Against Premature Peeling Failure of RC Beams with Externally Bonded Steel or FRP Plates", *Magazine of Concrete Research*, 2001, 53, 4, pp 251-262.

[5] Malek, A. M., Saadatmanesh, H., and Ehsani, M. R. "Prediction of Failure Loads of R/C Beams Strengthened with FRP Plate due to Stress Concentration at Plate End." *ACI Structural Journal*, 95, 1, 1998, pp 142–152.

[6] Pimanmas, A., Pornpongsaroj, P., "Peeling Behaviour of Reinforced Concrete Beams Strengthened with CFRP Plates under Various End Restraints", *Magazine of Concrete Research*, 56, 2, 2004, pp 73 - 81.

[7] El-Mihilmy, M.T., and Tedesco, J.W., ''Analysis of Reinforced Concrete Beams Strengthened with FRP Laminates.'' *ASCE J. Struct. Eng.,* 126, 6, 2000, pp 684–691.

[8] Sebastian, W.M., ''Sensitivities of Strength and Ductility of Plated Reinforced Concrete Sections to Preexisting Strains.'' *ASCE J. Struct. Eng.,* 128, 5, 2002, pp 624–636.